

Vibrational spectrum and electron-phonon coupling of doped solid picene from first principles

Alaska Subedi and Lilia Boeri

Max Planck Institute for Solid State Research, Heisenbergstrasse 1, D-70569 Stuttgart

(Dated: November 29, 2018)

We study superconductivity in doped solid picene ($C_{22}H_{14}$) with linear response calculations of the phonon spectrum and electron-phonon (ep) interaction. We show that the coupling of the high-energy C bond-stretching phonons to the π molecular orbitals for a doping of ~ 3 electrons per picene molecule is sufficiently strong to reproduce the experimental T_c of 18 K within Migdal Eliashberg theory. For hole doping, we predict a similar coupling leading to a maximum T_c of 6 K. However, we argue that, due to its molecular nature, picene may belong to the same class of strongly correlated ep superconductors as fullerenes. We propose several experimental tests for this hypothesis and suggest that intercalated hydrocarbons with different arrangements and numbers of benzene rings may be used to study the interplay between ep interaction and strong electronic correlations in the highly non-adiabatic limit.

PACS numbers: 31.15.A-, 74.70.Kn, 63.20.kd

The field of superconductivity has witnessed several important discoveries in the last ten years that, together with new synthesis and manipulation techniques, have enormously advanced our understanding of this phenomenon. These include MgB_2 with T_c of 39 K,[1] boron-doped diamond with T_c as high as 11.5 K,[2] intercalated graphite[3] with a T_c of 14.5 under pressure,[4] and iron based superconductors[5] with T_c of up to 56 K.[6] However, in order to be able to design superconductors with desired properties, additional efforts are needed to understand and control the material parameters relevant for superconductivity in different classes of compounds.

Carbon based compounds offer many possibilities in this regard because their structure can be easily manipulated at the atomic level and they generally possess high phonon frequencies that have substantial electron-phonon (ep) coupling. Besides many conventional phonon-mediated superconductors, this class also comprises alkali-intercalated fullerenes (A_3C_{60}) with T_c of up to 40 K.[7, 8] These π -bonded molecular solids have a rich phase diagram determined by a non-trivial interplay between strong local ep interactions and on-site Coulomb correlations in a highly non-adiabatic regime. [9–11] The physics of this strongly correlated ep superconductors is of great fundamental interest. Therefore, identifying other compounds in this class is highly desirable. For this reason, the discovery of superconductivity in K and Rb doped picene with T_c of up to 18 K by Mitsuhashi *et al.* last year[12] is of great significance.

In this paper, we use linear response calculations of the phonon spectra and ep interaction [13] within the rigid band approximation (RBA) to show that alkali-doped picene could be another case of strongly correlated ep superconductors. Our results complement previous theoretical and experimental studies of this compounds, which have focused on electronic properties and correlations.[17–23] We obtain a value of the ep coupling

constant that is large enough to explain superconductivity with $T_c = 18$ K in Migdal-Eliashberg theory. However, since the bandwidths of the conduction and valence bands in solid picene are relatively small (~ 0.3 – 1 eV), we argue that a local approach that includes both the ep coupling and Coulomb correlations on an equal footing may be more appropriate and also provide parameters that are relevant to these type of models. Finally, we discuss possible experimental tests that could confirm or exclude the scenario we propose.

Picene ($C_{22}H_{14}$) is a polycyclic aromatic hydrocarbon formed by five benzene rings juxtaposed in an arm-chair arrangement. Solid picene is an insulator, with a gap of ~ 3.3 eV, which can form in either monoclinic or orthorhombic structure.[24] Since the superconducting samples of Ref. 12 have a monoclinic $P2_1$ structure, we employed experimental lattice parameters for undoped picene in this variant with $a = 8.480$, $b = 6.154$, $c = 13.515$ Å, $\beta = 90.46^\circ$. [25] We relaxed the internal coordinates so that every component of force was less than 10^{-4} Ry/au. This changed the C-C and C-H bond lengths by less than 2.5% and was needed in order to have a dynamically stable structure with real phonon frequencies. [26] The unit cell contains two picene molecules placed in a herringbone arrangement in the xy plane (shown in the inset of Fig. 1) which are then stacked along z direction. The shortest intermolecular C-C distance is 3.5 Å within the xy plane and 3.9 Å along z (i.e. along the length of the picene molecule). These intermolecular distances are more than twice the typical intramolecular nearest-neighbour C-C distance of 1.4 Å. In the doped superconducting crystals, the a axis expands while the b and c axes shrink. It is inferred from this that the dopants most likely occupy intra-layer positions since inter-layer intercalation would have caused the c axis to expand. However, the detailed experimental structure of doped picene is not available. For this reason, we simulated

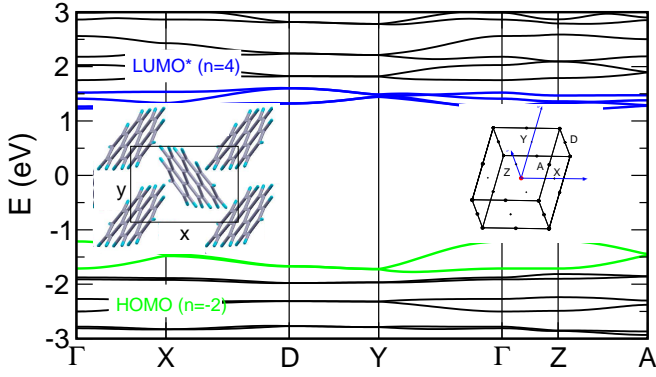


FIG. 1: (Color online) Calculated LDA electronic structure of solid picene. In green (light gray) and blue (dark gray) we show the two HOMO and the four LUMO* derived bands, respectively, which are accessible by hole or electron doping. n is the maximum number of electrons per picene molecule that can be doped. The two insets show the unit cell of solid picene in the xy plane and its Brillouin Zone (BZ), respectively.

the effect of doping using the rigid band approximation (RBA) and did not include explicitly the dopants in the calculations. The role of the dopant, which should be minor, is discussed in relation to graphite intercalated compounds (GIC).

The resulting electronic structure, which agrees well with previous density functional theory calculations,[17, 19, 20, 22] is shown in the main panel of Fig. 1. The zero of the energy in the figure is chosen as the middle of the calculated ~ 2.4 eV gap that separates the bonding valence bands from the anti-bonding conduction bands in undoped picene. All bands in the energy range shown in the figure have mostly C p_z character. They are lumped into small subsets with very small in- and out-of-plane dispersion reflecting the molecular nature of the solid. This is similar to the electronic structure of fullerenes whose conduction bands also have C p_z character and are very narrow.[9] In superconducting picene (K/Rb₃C₂₂H₁₄) the ~ 3 electrons donated from the alkali atoms to each molecule populate the 4 bands immediately above the gap. The Fermi surface (not shown) is large without any significant two-dimensional nature and prominent nesting features.[17, 21] These bands have a total bandwidth of ~ 0.3 eV [23] and derive from a combination of the two lowest unoccupied molecular orbitals (LUMO and LUMO+1), which have a small energy separation of ~ 66 meV in the molecule.[17] The energy separation between the two highest occupied molecular orbitals (HOMO and HOMO-1) is instead higher (~ 170 meV) so that the four corresponding bands in the solid are grouped in two subsets of two bands separated by a gap of ~ 0.1 eV. [17] In the following, we will study within RBA the effect of doping electrons or holes into the states immediately above (LUMO*) and below (HOMO) the gap, which are colored in blue and green, respectively, in

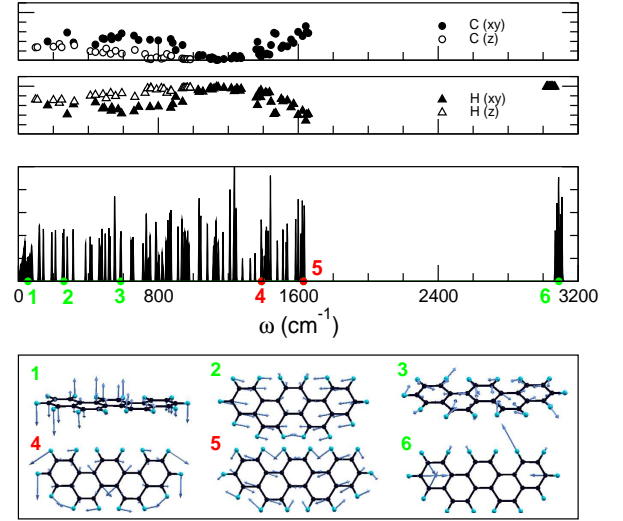


FIG. 2: (Color online) Vibrational properties of picene. *From top to bottom:* Partial C and H contribution to the phonon eigenvectors of a picene molecule. Phonon DOS of (undoped) solid picene with numbers that mark the energy position of selected modes, whose Γ -point eigenvectors are shown in the bottom panel. For clarity, only one picene molecule is shown. Modes 4 and 5 give the highest contribution to the ep coupling, shown in Fig. 3.

Fig. 1.

For all dopings, we will use the phonon spectrum of undoped solid picene, whose properties are summarized in Fig. 2. Most of the phonon branches of solid picene (not shown) have very little dispersion, which reflects the molecular nature of the solid. The dispersive inter-molecular modes (acoustic, translations and rotations of picene molecules) make up most of the phonon Density of States (DOS) for frequencies below ~ 85 cm^{-1} . The remaining modes are intramolecular vibration of C and H atoms and their general character can be inferred from the top two panels of Fig. 2, which show the calculated partial eigenvectors of an isolated picene molecule. The modes below ~ 800 cm^{-1} are due to in- and out-of-plane vibrations involving both C and H atoms that cause only small changes in the bond length between neighbouring atoms. Representative examples are shown in the bottom panel of Fig. 2. They are out-of-plane modes that bend picene molecules with frequency of ~ 55 cm^{-1} (1) and breathing modes with frequencies of ~ 260 (2) and ~ 585 cm^{-1} (3). At higher frequencies, the vibrational modes cause significant change of C-C and C-H bond lengths of adjacent atoms. The vibrations between ~ 800 cm^{-1} and ~ 1300 cm^{-1} are mostly out-of-plane, while the modes between ~ 1300 cm^{-1} and ~ 1600 cm^{-1} have C-H bending and C-C bending and stretching character. Two typical examples of such modes are shown in (4) and (5), with frequencies of ~ 1390 and ~ 1625 cm^{-1} , respectively. The spectral distribution of modes in this region is very simi-

lar to that of graphene and (intercalated) graphites. The modes very high in energy ($\sim 3200 \text{ cm}^{-1}$) have in-plane C-H bond stretching character as shown in (6).

The results of our *ep* calculations for hole and electron doped picene are summarized in Fig. 3. Even using the rigid band approximation, obtaining a reliable estimate of the coupling is far from trivial because the size of the system is large. However, the molecular nature of solid picene makes it possible to use additional approximations, which made the calculations feasible. In normal metals, the interaction between phonons and electrons is normally expressed in terms of Eliashberg spectral function:

$$\alpha^2 F(\omega) = \sum_{\mathbf{k}, \mathbf{q}, \nu, n, m} \frac{\delta(\epsilon_{\mathbf{k}}^n) \delta(\epsilon_{\mathbf{k}+\mathbf{q}}^m)}{N(E_F)} |g_{\mathbf{k}, \mathbf{k}+\mathbf{q}}^{\nu, n, m}|^2 \delta(\omega - \omega_{\nu \mathbf{q}}), \quad (1)$$

where $g_{\mathbf{k}, \mathbf{k}+\mathbf{q}}^{\nu, n, m}$ are the *ep* matrix elements that are averaged on the Fermi surface $\delta(\epsilon_{\mathbf{k}}^n)$. Its first inverse moment, $\lambda = 2 \int_0^\infty d\omega \alpha^2 F(\omega) / \omega$, gives the total *ep* coupling that appears in the exponent of the McMillan formula for the critical temperature T_c of *ep* superconductors. Evaluating expression (1) requires a careful integration in reciprocal space over a dense set of phonon (\mathbf{q}) and electron (\mathbf{k}) wavevectors even for elemental metals. However, we could obtain well converged results for λ and $\alpha^2 F(\omega)$ using affordable \mathbf{q} and \mathbf{k} meshes by exploiting the molecular nature of solid picene. First, we found the \mathbf{q} dependence of λ and $\alpha^2 F(\omega)$ to be weak, reflecting the molecular nature of solid picene. Indeed, the *ep* matrix elements g are essentially intramolecular quantities. Additionally, if the Fermi surface is not pathological, the integration over \mathbf{k} and \mathbf{q} in Eq. 1 can be done separately. The dimensionless *ep* coupling parameter λ can then be factorized as $\lambda = N(E_F) V_{ep}$, where the density of states $N(E_F)$ is determined by intermolecular interactions and the *ep* coupling strength V_{ep} is essentially an intramolecular quantity.[28, 29] Similarly, it is possible to define a spectral function for the *ep* coupling strength V_{ep} , $\bar{\alpha}^2 F(\omega) = \alpha^2 F(\omega) / N(E_F)$. The two intramolecular quantities $\bar{\alpha}^2 F(\omega)$ and V_{ep} converge much faster as a function of \mathbf{k} -mesh than the intermolecular $N(E_F)$. To eliminate the noise coming from pathological regions of the DOS, we evaluated V_{ep} and $\bar{\alpha}^2 F(\omega)$ for different fillings x of the electronic bands as shown in the two insets of Fig. 3.[30]

The values of V_{ep} thus determined are fairly constant with x within a single subset of bands, as one would expect for an intramolecular quantity. We obtain $V_{ep} = 150 \pm 20 \text{ meV}$ for holes and $V_{ep} = 110 \pm 5 \text{ meV}$ for electrons. This value of coupling is in reasonable agreement with the empirical trend $V_{ep} = 1800 / N_\pi$, where N_π is the number of atoms involved in π states, that has been estimated in C π bonded molecular systems. [29]

Before discussing the implications for superconductivity, it is insightful to analyze the V_{ep} spectral function

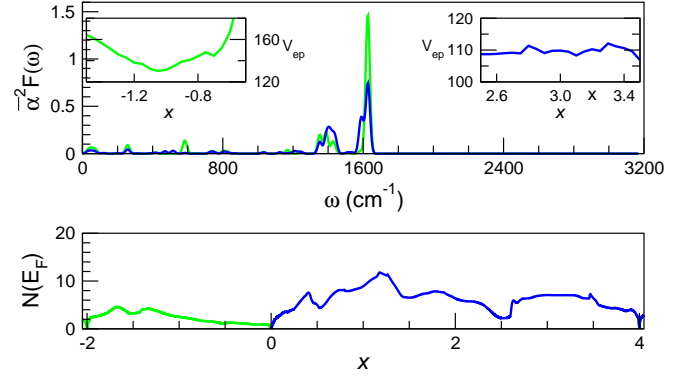


FIG. 3: (Color online) *Upper Panel*: Spectral distribution of the *ep* matrix elements of solid picene, doped with holes (green/light gray) or electrons (blue/dark gray). The two insets show the doping dependence of the corresponding *ep* coupling strength $V_{ep} = \int \omega^{-1} \alpha^2 F(\omega) d\omega$ for different values of doping x . *Lower Panel*: Electronic DOS per picene molecule, in states/(eV spin) as a function of doping x . The total *ep* coupling constant λ as a function of doping is given by $\lambda(x) = N(x) V_{ep}$.

$\bar{\alpha}^2 F(\omega)$, which is shown in the upper panel of Fig. 3. The *ep* spectral function has two main peaks at $\sim 1400 \text{ cm}^{-1}$ and $\sim 1600 \text{ cm}^{-1}$, which correspond to modes that bend C-H bonds and stretch C-C bonds (modes 4 and 5 in Fig. 2). Additionally, we also find smaller coupling to modes with lower frequencies ($\omega < 800 \text{ cm}^{-1}$). This spectral distribution is in agreement with the model calculations, [33] which also predict a sizable contribution at $\sim 260 \text{ cm}^{-1}$ that is present but reduced in our full-linear response calculation. [34]

The effect of the dopants on *ep* coupling, which is not explicitly included in our calculations, can be estimated from the comparison with graphite intercalation compounds. The intercalants in GICs partially reduce the *ep* coupling to C bond stretching modes, but also provide some additional coupling to low-lying Einstein phonons. [35–37] These two effects balance each other to leave λ basically unchanged, while ω_{ln} is reduced due to the additional weight at low frequencies. In contrast to GICs, which have substantial intercalant character for states near the Fermi level, both effects should be much weaker in solid picene because the metal states are not expected to significantly hybridize with C p_z states near the Fermi level. [18, 23]

Accurate values of $\lambda = V_{ep} N(E_F)$ as a function of doping can be obtained using the DOS shown in the lower panel of Fig. 3, which has been obtained using a $(8)^3$ \mathbf{k} -grid and tetrahedron method. [38] For $x = 3$, we get $N(E_F) = 7.06 \text{ states spin}^{-1} \text{ eV}^{-1}$, $\lambda = 0.78$ and $\omega_{\text{ln}} = 1021 \text{ cm}^{-1}$. Using $\mu^* = 0.12$ in the McMillan formula, we obtain a critical temperature $T_c = 56.5 \text{ K}$. This is more than three times the experimental value of T_c , and we need to use a larger value of $\mu^* = 0.23$ to reproduce the

experimental T_c . In the case of hole doping, the T_c 's are lower due to smaller values of DOS. For $x \sim -1.33$, with the same value of $\mu^* = 0.23$, $N(E_F) = 4.31$ states $\text{spin}^{-1} \text{eV}^{-1}$, $\lambda = 0.65$ and $\omega_{\text{ln}} = 890 \text{ cm}^{-1}$, and we obtain a maximum T_c of 6 K.

This relatively high McMillan T_c 's that result from strong ep coupling to a few high-energy C bond-stretching phonons indicates that superconductivity in alkali-doped picene and other hydrocarbons is most likely phonon-mediated, and related to that of other C and B-based superconductors such as MgB_2 , boron-doped diamond, and GICs.

However, the estimates of T_c based on Migdal-Eliashberg theory must be taken with care in the case of picene. In fact, we have shown that the bandwidth of the conduction bands ($W \sim 300 \text{ meV}$ for electrons and $\sim 1 \text{ eV}$ for holes), the frequencies of strongly coupled phonons ($\omega_{ph} \sim 200 \text{ meV}$), the ep coupling strength ($V_{ep} \sim 110\text{-}150 \text{ eV}$) and Coulomb repulsion ($U \sim 1.2 \text{ eV}$ [22]) all have similar magnitudes. In this range of parameters, the two most important approximations in Migdal-Eliashberg theory of superconductivity, Migdal's theorem and the Morel-Anderson scheme for the screening of the Coulomb repulsion, may be invalid. In fullerenes, whose conduction electrons have C p_z character, this regime of parameters gives rise to a variety of interesting phenomena, the most spectacular being the occurrence of ep superconductivity near a Mott insulating phase, [39] well captured by theoretical studies of local models of interacting phonons and electrons in the non-adiabatic regime.[9–11]

Intercalated picene is also a strong candidate for this kind of strongly correlated, non-adiabatic ep superconductivity. The experimental situation is still premature to verify this claim, but several tests are possible for this hypothesis. For example, Migdal-Eliashberg theory would predict a smooth behaviour of superconductivity as a function of doping and pressure that is governed essentially by the value of the electronic DOS at the Fermi level. On the other hand, strongly correlated local models would predict a phase diagram where superconductivity exists in close proximity to a possible Mott insulating state, which could be tuned by doping or by a change in the intermolecular hopping driven by pressure or intercalation of isovalent atoms with different sizes. A very exciting prospect is the possibility of studying a wider range of intercalated hydrocarbons by changing the number and arrangement of benzene rings. This could be an interesting avenue for independently tuning the ep coupling [29] and bandwidth and degeneracy of the conduction bands and obtaining an extensive mapping of the parameter space for strongly correlated ep superconductors.

In summary, we report the results of our first principles calculations for the vibrational spectrum and ep coupling of doped solid picene within the rigid band approxima-

tion. We find a large coupling of bond-stretching phonons at $\sim 1400 \text{ cm}^{-1}$ and $\sim 1600 \text{ cm}^{-1}$ both to electrons in the four lowest conduction bands and holes in the two highest valence bands of solid picene ($V_{ep} \sim 110$ and 150 meV , respectively). This is sufficiently strong to explain the experimental T_c of 18 K reported for $\text{K}_3\text{C}_{22}\text{H}_{14}$ within the Migdal Eliashberg theory for ep superconductors. However, due to the molecular nature of solid picene, we argue that a strongly correlated non-adiabatic ep superconductivity similar to that of alkali-doped fullerenes may occur. We propose possible experimental tests of this hypothesis and suggest that alkali-intercalated hydrocarbons may be ideal playgrounds to study the interplay between electronic and vibrational energy scales in a controlled way.

We would like to thank O. Gunnarsson, R. Arita and S. Ciuchi for useful discussion. L.B. acknowledges hospitality of the KITP, Santa Barbara, where part of this work was carried out.

Recently a T_c of 5 K was reported in K-doped phenanthrene ($\text{C}_{14}\text{H}_{10}$), [40] confirming the possibility of observing superconductivity in other polycyclic aromatic hydrocarbons.

Note added: We have become aware of a paper by Casula *et al.* that studies electron-phonon coupling in $\text{K}_3\text{C}_{22}\text{H}_{14}$. [31] They integrate over full phonon spectrum and find $\lambda = 0.88$ and $\omega_{\text{ln}} = 202 \text{ cm}^{-1}$. With the caveat that our low frequency modes are less converged, if we also integrate over the full phonon spectrum, we obtain $\lambda = 1.41$ and $\omega_{\text{ln}} = 240.18 \text{ cm}^{-1}$. The discrepancy in the value of λ may be because our value of DOS (7.06 states $\text{spin}^{-1} \text{eV}^{-1}$ per molecule) is more than twice larger than theirs (6.2 states $\text{spin}^{-1} \text{eV}^{-1}$ per cell = 3.1 states $\text{spin}^{-1} \text{eV}^{-1}$ per molecule).

-
- [1] J. Nagamatsu, N. Nakagawa, T. Muranaka, Y. Zenitani and J. Akimitsu, *Nature* **410**, 63 (2001).
 - [2] E.A. Ekimov, V.A. Sidorov, E.D. Bauer, N.N. Mel'nik, N.J. Curro, J.D. Thompson, and S.M. Stishov, *Nature* **428**, 542 (2004).
 - [3] T. E. Weller, M. Ellerby, S. S. Saxena, R. P. Smith, and N. T. Skipper, *Nature Physics* **1**, 39 (2005).
 - [4] N. Emery, C. Hérold, M. d'Astuto, V. Garcia, Ch. Bellin, J. F. Maréché, P. Lagrange, and G. Loupias, *Phys. Rev. Lett.* **95**, 087003 (2005).
 - [5] Y. Kamihara, T. Watanabe, M. Hirano, and Hideo Hosono, *J. Am. Chem. Soc.* **130**, 3296 (2008).
 - [6] C. Wang, L. Li, S. Chi, Z. Zhu, Z. Ren, Y. Li, Y. Wang, X. Lin, Y. Luo, S. Jiang, X. Xu, G. Cao and Z. Xu, *Europhys. Lett.* **83**, 67006 (2008).
 - [7] A.F. Hebard, M.J. Rosseinsky, R.C. Haddon, D.W. Murphy, S.H. Glarum, T.T.M. Palstra, A.P. Ramirez, and A.R. Kortan, *Nature* **350**, 600 (1991).
 - [8] T.T.M. Palstra, O. Zhou, Y. Iwasa, P.E. Sulewski, R.M. Fleming, and B.R. Zegarski, *Solid State Commun.* **93**, 327 (1995).

- [9] O. Gunnarsson, *Alkali-Doped Fullerenes* (World Scientific, Singapore, 2004).
- [10] M. Capone, M. Fabrizio, C. Castellani, and E. Tosatti, *Rev. Mod. Phys.* **81**, 943 (2009).
- [11] C. Grimaldi, L. Pietronero, and S. Strssler, *Phys. Rev. Lett.* **75**, 1158 (1995).
- [12] R. Mitsunashi, Y. Suzuki, Y. Yamanari, H. Mitamura, T. Kambe, N. Ikeda, H. Okamoto, A. Fujiwara, M. Yamaji, N. Kawasaki, Y. Maniwa, and Y. Kubozono, *Nature* **464**, 76 (2010).
- [13] The results presented here are obtained using density functional perturbation theory[14] within the local density approximation (LDA) as implemented in the Quantum-Espresso package.[15] We employed norm-conserving pseudopotentials[16] and a plane wave basis set with a cut-off of 70 Ry. Dynamical matrices were calculated on a $(2)^3$ grid in reciprocal (\mathbf{q} -space), and phonon dispersions and DOS were then obtained by Fourier transformation of the real-space force constants. For the self-consistent calculations of phonon frequencies, we employed a $(2)^3$ grid in \mathbf{k} -space.
- [14] S. Baroni, S. de Gironcoli, A. Dal Corso, and P. Gianozzi, *Rev. Mod. Phys.* **73**, 515 (2001).
- [15] P. Gianozzi, S. Baroni, N. Bonini, M. Calandra, R. Car, C. Cavazzoni, D. Ceresoli, G. L. Chiarotti, M. Cococcioni, I. Dabo *et al.*, *J. Phys.: Condens. Matter* **21**, 395502 (2009).
- [16] We used the pseudopotentials C.pz-vbc.UPF and H.pz-vbc.UPF from <http://www.quantum-espresso.org>.
- [17] T. Kosugi, T. Miyake, S. Ishibashi, R. Arita, and H. Aoki, *J. Phys. Soc. Jpn.* **78**, 113704 (2009).
- [18] H. Okazaki, T. Wakita, T. Muro, Y. Kaji, X. Lee, H. Mitamura, N. Kawasaki, Y. Kubozono, Y. Yamanari, T. Kambe, T. Kato, M. Hirai, Y. Muraoka, and T. Yokoya, *Phys. Rev. B* **82**, 195114 (2010).
- [19] F. Roth, M. Gatti, P. Cudazzo, M. Grobosch, B. Mahns, B. Büchner, A. Rubio, and M. Knupfer, *New J. Phys.* **12**, 103036 (2010).
- [20] P.L. de Andres, A. Guijarro, and J.A. Vergés, *arXiv:1010.6168*.
- [21] M. Kim, B.I. Min, G. Lee, H.J. Kwon, Y.M. Rhee, and J.H. Shim, *Phys. Rev. B* **83**, 214510 (2011).
- [22] G. Giovannetti, and M. Capone, *Phys. Rev. B* **83**, 134508 (2011).
- [23] F. Roth, B. Mahns, B. Büchner, and M. Knupfer, *Phys. Rev. B* **83**, 144501 (2011).
- [24] H. Okamoto, N. Kawasaki, Y. Kaji, Y. Kubozono, A. Fujiwara, and M. Yamaji, *J. Am. Chem. Soc.* **130**, 10470 (2008).
- [25] A. De, R. Ghosh, S. Roychowdhury, and P. Roychowdhury, *Acta Cryst. C* **41**, 907 (1985).
- [26] Along the interlayer stacking direction $(0,0,1)$, two acoustic phonon modes still have small imaginary frequencies of -12.7 and -7.8 cm^{-1} near the zone boundary. Convergence of these low-energy acoustic modes is a well-known problem also in graphite-related systems and can require very large plane-wave cutoffs[27], which are prohibitive in this case. However, we find that all intramolecular modes are well converged with accuracies of ~ 1 %.
- [27] N. Mounet and N. Marzari, *Phys. Rev. B* **71**, 205214 (2005).
- [28] M. Lannoo, G.A. Baraff, M. Schlüter, D. Tomanek, *Phys. Rev. B* **44**, 12106 (1991).
- [29] A. Devos, and M. Lannoo, *Phys. Rev. B* **58**, 8236 (1998).
- [30] As we are focusing only on the intramolecular modes, we ignore the coupling of electrons to phonon frequencies below 100 cm^{-1} when we integrate $\alpha^2 F(\omega)$. If we integrate over the full phonon spectrum (while keeping in mind that our low frequency acoustic phonons are less converged), we get $\lambda = 1.41$ and $\omega_{\text{in}} = 240.18$ cm^{-1} . Using $\mu^* = 0.12$, this again gives comparable $T_c = 35.86$ K. Note also that the inter- and intra-molecular phonons, which play very different roles in the transport properties of organic crystals, should also play different roles in superconductivity due to the different adiabatic ratio.[32].
- [31] M. Casula, M. Calandra, G. Profeta, and F. Mauri *arXiv:1106.1446*.
- [32] S. Ciuchi and S. Fratini, *Phys. Rev. Lett.* **106**, 166403 (2011).
- [33] T. Kato, K. Yoshizawa, and K. Hirao, *J. Chem. Phys.* **116**, 3420 (2002).
- [34] Consistently, Kato *et al.* get larger values also of the coupling constant ($V_{ep} = 180$ meV). The most likely reason for this discrepancy is that our calculations take into account the real band structure and electronic screening of the solid, while the calculation of Ref. 33 are based on a molecular model that includes only the LUMO orbital.
- [35] M. Calandra and F. Mauri, *Phys. Rev. Lett.* **95**, 237002 (2005).
- [36] Lilia Boeri, Giovanni B. Bachelet, Matteo Giantomassi, and Ole K. Andersen, *Phys. Rev. B* **76**, 064510 (2007).
- [37] J. S. Kim, L. Boeri, J. R. O'Brien, F. S. Razavi, and R. K. Kremer *Phys. Rev. Lett.* **99**, 027001 (2007).
- [38] P.E., Blöchl, O. Jepsen and O.K. Anderson, *Phys. Rev. B* **49**, 16223 (1994).
- [39] A.Y. Ganin, Y. Takabayashi, Y.Z. Khimyak, S. Margadonna, A. Tamai, M.J. Rosseinsky, and K. Prassides, *Nature Materials* **7**, 367 (2008).
- [40] X.F. Wang, R.H. Liu, Z. Gui, Y.L. Xie, Y.J. Yan, J.J. Ying, X.G. Luo, X.H. Chen, *arXiv:1102.4075*.